Foot Placement and Velocity Control in Smooth Bipedal Walking

Eric R. Dunn Robert D. Howe

Division of Applied Sciences
Harvard University
Cambridge, Massachusetts 02138

Abstract

For a walking robot to negotiate rough terrain it must adjust its step length to hit suitable footholds while simultaneously regulating its forward speed. This paper develops an algorithm to achieve these aims for a planar dynamic biped in the context of smooth exchange of support. The basis of the algorithm is an asymmetric gait to adjust walking velocity combined with a set of conditions on the leg lengths which ensure smooth exchange of support for any step size. The algorithm was tested on level surfaces in simulation and on an experimental biped robot. The algorithm could track a 30% change in desired walking velocity and a 25% change in desired step length.

1 Introduction

Animals walk, but most man-made vehicles roll. On prepared surfaces, wheels are smooth: they enable locomotion with minimal disturbance to the payload. This allows us to ride comfortably in automobiles at high speeds, and indeed a "smooth ride" is a key attribute of a luxury car. Unfortunately, wheeled vehicles lose the ability to move smoothly when the ground is not regular, and on very rough terrain they cannot move at all. On these difficult surfaces legged locomotion becomes a winning alternative, because it permits arbitrary placement of the feet to avoid obstacles. Animals can move over extremely rugged terrain; the ability of goats to climb steep mountain sides is legendary, and humans routinely negotiate steep stairs and ladders. This motion is not smooth, however, even on level ground, since legged locomotion in many animals optimizes energy efficiency rather than smoothness [1].

Our research is aimed at understanding how to build robots that preserve the advantages of legs and simultaneously walk smoothly. In previous work [2], we considered the fundamental problem of smooth exchange of support for a simple planar bipedal robot. There we derived a set of conditions on leg lengths which ensure that the robot's body does not experience an instantaneous change in velocity as the robot's weight is transferred from one leg to the other. Here we consider methods to control other essential parameters of gait.

Hodgins [3] noted that in order for a legged robot to negotiate rough terrain, it must select a series of suitable footholds and then choose its step length to attain those footholds. During this process the robot must also regulate its forward speed. We propose an algorithm which permits the independent control of step length and walking velocity, while still satisfying the smooth exchange of support criteria to ensure that smooth locomotion is maintained. To investigate the efficacy of our new algorithm we examine its performance in simulation and on our experimental hardware. In this paper, we examine walking on only flat, level surfaces. Our algorithm, however, provides a basis for walking on more difficult terrain.

Raibert, Hodgins, and their colleagues [3, 4, 5] examined the problems of foot placement and forward velocity control for their running robots. These remarkable machines can run, hop, negotiate stairsteps, and even somersault, but the objective of these machines is not smooth motion, and the running gaits they employ are not smooth. Kajita and his coworkers [6, 7] built a series of bipedal robots with control algorithms that minimize excursions of the robots' bodies, but their goal was to simplify the dynamics of the system, rather than create a smooth walk. Blajer and Schiehlen [8] have examined impact-free walking of a complex biped from a theoretical point of view. None of the foregoing studies have aimed at the the development of smooth walking over uneven ground.

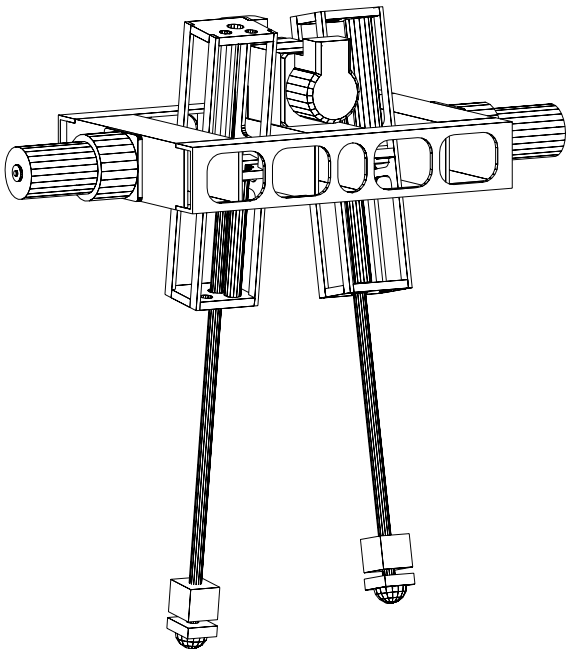

Figure 1: An experimental planar five-link walking biped.

2 Experimental hardware

We believe that experimental verification of our control strategies is essential, and consequently, we have constructed a planar bipedal robot to serve as the test bed for our research. Figure 1 shows the machine's basic structure, which consists of a pair of legs joined to a body. Each leg pivots on a rotary hip joint at the body and contains a prismatic lower leg joint which acts to change the leg length.

Pneumatic cylinders drive the extension and retraction of the lower legs. We selected pneumatic cylinders for this application because of their favorable force to weight ratio. Unfortunately, continuous control of pneumatic systems is notoriously difficult (see [9], for example), and we found it necessary to implement a nonlinear observer-based control scheme to obtain reasonable performance under walking conditions. The hip joints are driven by conventional DC servomotors with harmonic drive gearheads.

Force sensors near the hemispherical feet transduce ground reaction forces, and potentiometers at the joints permit measurement of the robot's configuration and orientation. The robot stands about 35 cm high and weighs approximately 5.6 kg. A boom mechanism (not shown) constrains the motions of the robot to the sagital plane, simplifying the problem of balance and eliminating out of plane considerations.

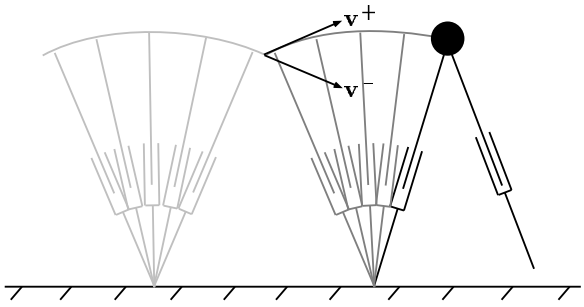

Figure 2: The compass gait. During single support, the hip follows the arc of a circle with radius equal to the stance leg length. At exchange of support, there is an instantaneous change in linear velocity of the hip.

3 Smoothing bipedal walking

A step in the gait of a dynamic biped consists of two phases: *(a)* a single support phase in which one leg is in contact with the ground and the other leg is not, and *(b)* an exchange of support during which the legs trade roles. In the single support phase, the *stance leg* is in contact with the ground and carries the weight of the biped, while the *swing leg* usually moves forward in preparation for the next step. At exchange of support the weight of the robot is transferred from one leg to the other. In this section, we examine exchange of support, discuss why it might not be smooth, and present a set of constraints which ensure smooth exchange of support.

Inman *et al.* [10] examined bipedal walking in humans and proposed a model of bipedal walking based on the compass gait (Figure 2). In this gait the leg lengths are fixed, so the hip trajectory follows the arc of a circle as the biped pivots about the distal end of the stance leg. At exchange of support, the stance and swing legs trade roles, and the hip begins to follow the arc of a new circle. Because the origins of the two circles are not coincident, the hip trajectory contains a cusp at exchange of support. Velocity vectors $\mathbf{v}^-$ and $\mathbf{v}^+$ attached to the hip trajectory at a cusp indicate translational velocity of the hip just before and just after exchange of support, respectively. The two velocities are not equal ($\mathbf{v}^- \neq \mathbf{v}^+$), and the hip experiences an instantaneous change in velocity at exchange of support. A payload or passenger riding at the hip of the biped would experience this instantaneous change in velocity as an infinite acceleration with an accompanying impulse. The compass gait is certainly not smooth.

If we have control of the lengths of the legs, however, we can modify the compass gait to ensure smooth

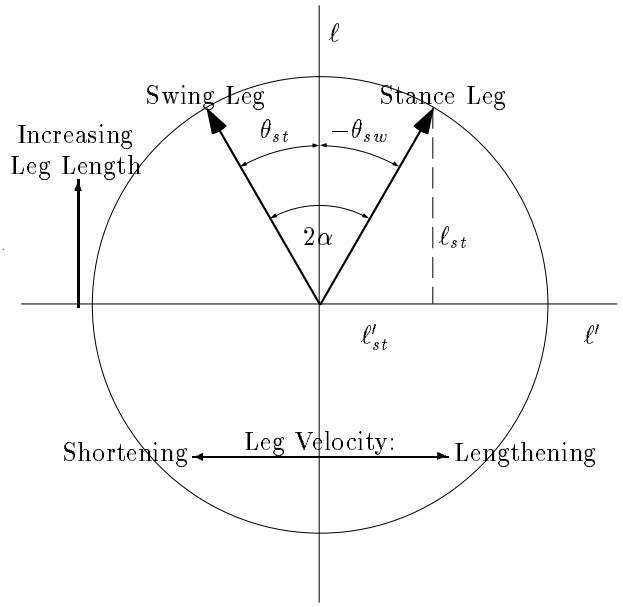

Figure 3: Phase diagram for smooth exchange of support. The diagram illustrates the relationship between the necessary stance and swing leg motions.

exchange of support. Specifically, we require that the velocity of the hip remains unchanged during exchange of support

$$\mathbf{v}^- = \mathbf{v}^+,$$

and then determine the leg lengths and velocities necessary to satisfy this condition. We presented a complete derivation of these conditions in a previous paper [2] and only summarize the results below.

Defining the terms of interest, let ℓ_{st} be the length of the stance leg, ℓ_{sw} be the length of the swing leg, θ_{st} be the angle of the stance leg with respect to gravity, θ_{sw} be the angle of the swing leg with respect to gravity, and let 2α be the angle between the legs ($2\alpha = \theta_{st} - \theta_{sw}$). With these definitions, the conditions for exchange of support with no velocity discontinuity are

$$\begin{bmatrix} \ell'_{sw} \\ \ell_{sw} \end{bmatrix} = \begin{bmatrix} \cos 2\alpha & -\sin 2\alpha \\ \sin 2\alpha & \cos 2\alpha \end{bmatrix} \begin{bmatrix} \ell'_{st} \\ \ell_{st} \end{bmatrix}, \quad (1)$$

$$\ell'_{st} + \ell_{st} \tan\theta_{sw} = 0, \quad (2)$$

where $(\cdot)'$ indicates a derivative with respect to θ_{st}.

To illustrate the geometrical meaning of Equations (1, 2), we use a phase diagram (Figure 3). The vertical axis in Figure 3 is leg length, and the horizontal axis is rate of change of leg length. In this diagram the length and rate of change of each leg is represented by a vector. From Equation (1), the relationship between legs' vectors is a simple rotation by 2α. Equation (2) fixes the angle of the stance leg's vector with respect to the vertical axis.

The significance of the phase diagram is that it determines the lengths and rate of change of the legs during exchange of support. For the particular "symmetric" configuration shown in Figure 3, we see that $\theta_{st} + \theta_{sw} = 0$. Since the leg vectors lie on a circle, the legs must be the same length at exchange of support. The rate of length change of the legs are equal but opposite, with the stance leg extending and the swing leg retracting. These coordinated actions eliminate any velocity discontinuity of the hip at exchange of support.

The phase diagram does not completely fix all gait parameters at exchange of support. In particular, the radius of the circle is a free parameter, allowing us to select the body height at exchange of support. The angle 2α is free which allows us to specify step length. Finally, either θ_{st} or θ_{sw} may be freely selected. We will use this degree of freedom to control the forward walking velocity of the biped.

4 Velocity control with asymmetry

Using a technique similar to the velocity control algorithm employed by Raibert [4] with his hopping robots, we seek to control the forward velocity of our walking robot by introducing an asymmetry to the walking gait. We define the gait asymmetry β as the difference between the stance leg angle and the swing leg angle at exchange of support,

$$\beta = \theta_{st} - (-\theta_{sw}). \quad (3)$$

When the gait is symmetric as in Figure 3, the stance phase begins with the body a particular distance behind the point of support, and ends with the body the same distance in front of the point of support. The body spends equal amounts of time in front of and behind the point of support, and the net acceleration due to gravity acting on the body is zero.

If we introduce a positive asymmetry to the gait, then θ_{st} increases, $-\theta_{sw}$ decreases, and the biped's body will spend less time behind the point of support than in front of it. Gravity will have more opportunity to accelerate than decelerate the body, and the result will be a net acceleration. Conversely, a negative asymmetry will result in a net deceleration.

Since the addition of an asymmetry in the gait produces velocity changes, our control algorithm closes

a feedback loop around forward velocity by setting the asymmetry proportional to the velocity error, $\beta = G(v_d - v)$, where v_d is the desired velocity, G is a feedback gain, and v is the measured walking velocity. Walking velocity may be determined by dividing the previous step length by the duration of that step, or estimated by examining the horizontal velocity of the hip during a step. In the simulations and experiments which follow, we define "forward velocity" to be horizontal velocity of the hip as it passes over the point of support.

The step length

$$L = \ell_{st} \sin\theta_{st} - \ell_{sw} \sin\theta_{sw}, \tag{4}$$

and body height at exchange of support

$$h = \ell_{st} \cos\theta_{st} = \ell_{sw} \cos\theta_{sw} \tag{5}$$

may be specified by the robot's operator or determined by a obstacle avoidance planner.

Combining Equations (3, 4, 5) we obtain

$$\tan\theta_{st} + \tan(\theta_{st} - \beta) = \frac{L}{h}.$$

This equation can be solved online with a few iterations of Newton's method to determine the gait parameter θ_{st}. The remaining gait parameters then follow from Equations (1, 2).

5 Implementations

To test the velocity and step length control algorithms developed in the previous section, we implemented the controller in simulation and on the experimental biped.

5.1 Simulation

For the purposes of simulation, we modeled the biped as an inverted pendulum with adjustable length legs. The model neglected swing leg rotational inertia and also assumed that the leg lengths and swing hip angle could be controlled exactly. In operation, the simulation begins with the body moving over the point of support with some initial velocity. With the body over the point of support, the velocity control algorithm compares the forward velocity to the desired forward velocity and computes a gait asymmetry based on the velocity error. Using this asymmetry, the body height, and the desired step length, the smooth exchange of support conditions are applied to obtain

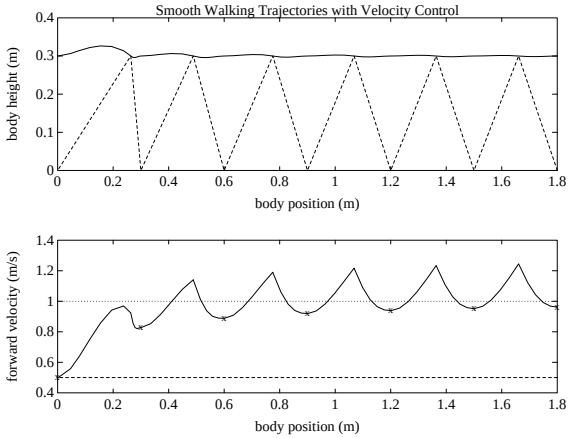

Figure 4: Velocity control algorithm applied to a biped in simulation. The upper plot is a trace of the horizontal and vertical location of the robot's hip. The location of the stance and swing legs at exchange of support are also indicated. The biped walks from left to right. The lower plot shows the forward velocity of the robot's hip. The robot begins with a forward velocity of 0.5 m/s, and the desired velocity is 1.0 m/s. Small x's indicate the midpoint of each stride, i.e. the point at which the hip is directly above the point of support.

θ_{st}, θ_{sw}, and the required leg lengths and velocities. A cubic spline trajectory is computed to drive the stance leg length to its target value, and then the model is integrated forward to exchange of support.

At exchange of support, the swing leg position and velocity are known, and are assigned to the new stance leg. A second cubic spline is computed for the stance leg length program, and the model is integrated forward to a point where the body is again over the point of support. At this stage, one step is complete. The simulation process repeats for additional steps.

In Figure 4 we show the results of one simulation. Here the robot begins with a forward velocity of 0.5 m/s and we ask that it accelerate to 1.0 m/s. In accordance with the velocity control algorithm, the gait begins with a large positive asymmetry, and the robot accelerates rapidly. By the midpoint of the second step, the forward velocity is greater than 0.8 m/s. On subsequent steps the forward velocity converges to the desired velocity, and the gait becomes more symmetrical.

An examination of the second plot in Figure 4 illustrates the effect of smooth exchange of support constraints. In this plot, we see that forward velocity is continuous across each exchange of support. We also note, however, that the velocity trajectory contains a cusp. That is, the *acceleration* is discontinuous.

The origin of this discontinuity is easy to understand. Just before exchange of support the point of support is behind the body and the body accelerates. Just after exchange of support the point of support is in front of the body and the body decelerates. Hence, our exchange of support conditions provide sufficient smoothing to eliminate infinite accelerations, but do not eliminate infinite *jerk.* An explicit double support phase during exchange of support could be used to provide additional smoothing. With both feet on the ground, the robot would be able to create a smooth transition across exchange of support. The transition would have to occur very rapidly to maintain dynamic walking. We will not consider double support further here, but consider it future work.

We also see in Figure 4 that in order to meet the conditions for smooth exchange of support, the robot must introduce a vertical component to the hip trajectory. There is a tradeoff between the reduction of velocity discontinuity at exchange of support and the addition of accelerations during other portions of the gait.

5.2 Experimental Implementation

To test our velocity and step length control algorithm on the experimental biped, we constructed a control panel from which an operator could adjust the value of desired step length or velocity while the robot walked. In the first of three experiments, the operator began with one desired speed and then increased the desired speed halfway through the walk. In the second experiment the operator decreased the desired walking speed during the walk. In the final experiment the operator adjusted the step length of the robot.

Figure 5 plots data taken from the first two experiments. In the first experiment, the initial desired velocity is 0.195 m/s. For the first dozen steps of the walk, the robot maintains a forward speed near the desired velocity. When the operator increases the walking speed by 30% to 0.257 m/s in the middle of the thirteenth step, the robot stumbles slightly, but then accelerates to near the new desired value. The step-to-step speed variation present in the data even when the operator commands a constant velocity is typical of this robot, and we believe that it is due primarily to joint control errors in the pneumatic legs.

The second plot in Figure 5 plots data from the second experiment, in which the operator decreases the desired velocity during the walk. We see that the robot's velocity decreases in response to the command, again with considerable step-to-step variation.

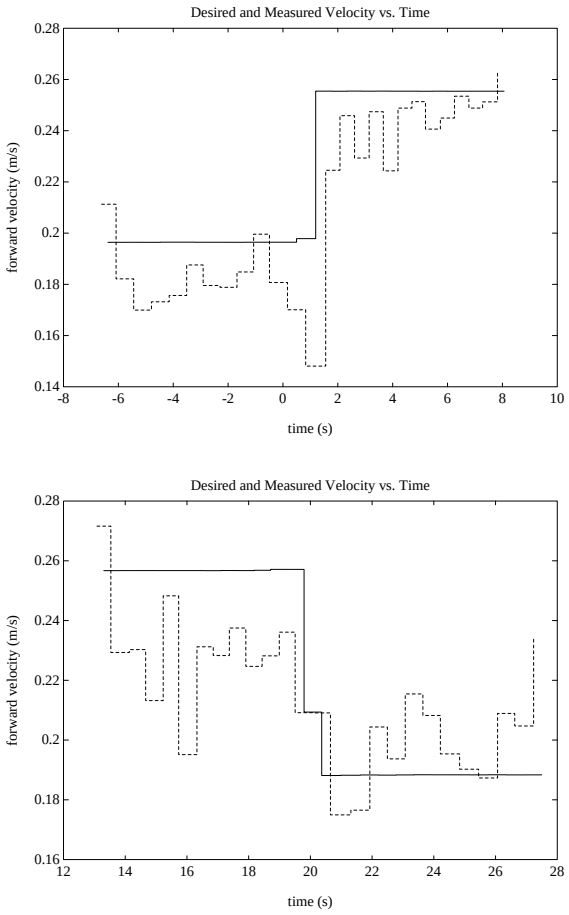

Figure 5: Velocity control algorithm applied to the experimental biped. The solid line is the desired forward velocity. The dashed line is the estimated forward velocity at each step.

We present data from the third experiment in Figure 6. In this experiment the operator increases the desired step length from about 0.15 m to 0.20 m during the walk. Since step length is just a kinematic condition in the algorithm, we expect the actual step length to track the desired step length very closely. The data confirms this expectation and we see the step length errors during the walk are just a few percent of the total step length, with the largest error being 7 mm.

Also shown in Figure 6 are the hip trajectories across five steps. At exchange of support, the hip appears to sag by as much as 5 mm, despite our efforts to smooth exchange of support. When the weight of the body in transferred, the pressure in the pneumatic cylinders must increases rapidly. We believe the hip sag is a result of saturation in the pneumatic valves as they try to rapidly increase the pressure in the leg.

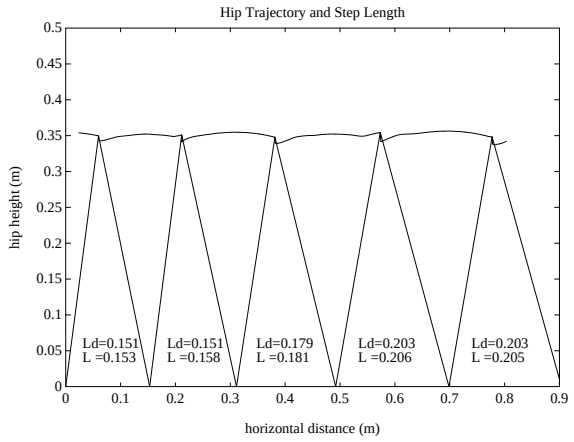

Figure 6: Hip trajectory and step length during a walk. The hip height shows some periodic variation around its nominal value of 0.35 m. The position of the stance and swing legs at each exchange of support is shown. The actual step length L is compared with the desired step length L_d. All lengths are in meters.

6 Conclusions

We have developed a control algorithm which can independently regulate the step length and forward walking velocity of a bipedal gait, while maintaining smooth exchange of support. In simulating the algorithm, we found that it is successful, within limits on the achievable smoothness. In experiments we again found that the algorithm is successful, but its authority and smoothness are limited by joint control errors. This algorithm enables the development of dynamic bipedal walkers which can walk smoothly, with well regulated velocity, while employing unevenly spaced footholds. In future work, we will apply this control scheme to rough terrain problems.

References

[1] R. McN. Alexander. The gaits of bipedal and quadrupedal animals. *International Journal of Robotics Research*, 3(2):49–59, Summer 1984.

[2] Eric R. Dunn and Robert D. Howe. Towards smooth bipedal walking. In *Proceedings of the IEEE International Conference on Robotics and Automation*, volume 3, pages 2489–2494, San Diego, May 1994.

[3] J. Hodgins. Legged robots on rough terrain: Experiments in adjusting step length. In *Proceedings of the IEEE International Conference on Robotics and Automation*, pages 824–826, April 1988.

[4] M. H. Raibert. *Legged Robots that Balance*. MIT Press, Cambridge, 1986.

[5] J. K. Hodgins and M. H. Raibert. Biped gymnastics. *International Journal of Robotics Research*, 9(2):115–132, April 1990.

[6] S. Kajita, T. Yamaura, and A. Kobayashi. Dynamic walking control of a biped robot along a potential energy conserving orbit. *IEEE Transactions on Robotics and Automation*, 8(4):431–438, August 1992.

[7] S. Kajita and K. Tani. Study of dynamic biped locomotion on rugged terrain. In *Proceedings of the IEEE International Conference on Robotics and Automation*, pages 1405–1411, April 1991.

[8] W. Blajer and W. Schiehlen. Walking without impacts as a motion/force control problem. *Journal of Dynamics Systems, Measurement, and Control*, 114:660–665, December 1992.

[9] S. Liu and J. E. Bobrow. An analysis of a pneumatic servo system and its application to a computer-controlled robot. *ASME Journal of Dynamic Systems, Measurement, and Control*, 110:228–235, September 1988.

[10] V. T. Inman, H. J. Ralston, and F. Todd. *Human Walking*. Williams & Wilkins, Baltimore, 1981.